UCRL-JC-130942
PREPRINT

Hard X-ray Production from High Intensity Laser Solid Interactions

M. D. Perry, J. A. Sefcik, T. Cowan, S. Hatchett, A. Hunt,
M. Moran, D. Pennington, R. Snavely, S. C. Wilks

This paper was prepared for submittal to the
12th Topical Conference on High Temperature Plasma Diagnostics
Princeton, NJ
June 7-11, 1998

June 3, 1998

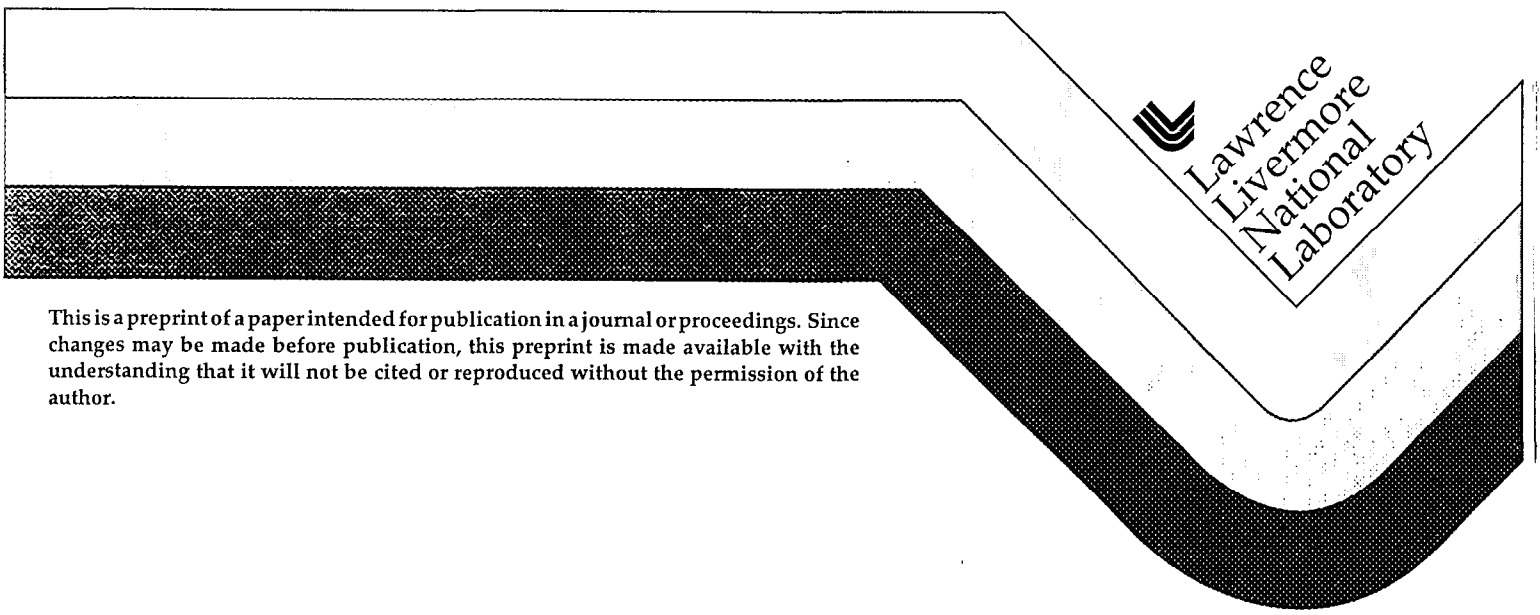

Hard x-ray production from high intensity laser solid interactions

M.D. Perry, J A Sefcik, T Cowan, S. Hatchett, A Hunt, M Moran, D Pennington,

R Snavely, and S C Wilks

Lawrence Livermore National Laboratory, Livermore, California 94550

Intense laser ($>10^{21}$ W/cm^2) driven hard x-ray sources offer a new alternative to conventional electron accelerator bremsstrahlung sources. These laser driven sources offer considerable simplicity in design and cost advantage for multiple axis views and have the potential for much higher spatial and temporal resolution than is achievable with accelerator sources We have begun a series of experiments using the Petawatt Laser system at LLNL to determine the potential of these sources for radiography applications Absolutely calibrated spectra extending to 20 MeV and high resolution radiographs through a $\rho r \geq 150$ gm/cm^2 have been obtained The physics of these sources and the scaling relationships and laser technology required to provide the dose levels necessary for radiography applications will be discussed Diagnostics of the laser produced electrons and photons will be addressed

I. INTRODUCTION

Electron beam accelerators are commonly used in ballistics research to assess the dynamic behavior of explosively driven systems The Lawrence Livermore National Laboratory uses the FXR facility at Site 300 to produce flash x-rays from an electron beam source The Dual-Axis Radiographic Hydrotest Facility under construction at Los Alamos National Laboratory will provide a two-axis view of fast moving objects with some ability to image with several exposures

The use of petawatt class lasers for the production of copious amounts of high energy x-rays has been discussed for over a decade [1,2] In fact, intermediate energy (0.1-1 MeV) x-ray production with table-top size terawatt class lasers

is now a sub-field within the strong field interaction community Numerous groups have observed electrons or bremsstrahlung spectra extending beyond 1 MeV [3,4,5,6]

Recent experiments on the Petawatt laser at the NOVA laser facility at LLNL have demonstrated the short (<1 psec) laser pulses, when properly focussed on high-z targets, can produce hard, intense x-ray spectra that can be used for radiography Scaling arguments suggest that a laser driven radiographic source could have a performance that rivals that of electron beam driven radiographic devices

II. RECENT EXPERIMENTS

Petawatt shots occurred during the week of September 5-10, 1997 Basic laser data was a pulse duration of 460 $\pm$ 40 fsec and a compressor throughput of 84% Typical laser energy measured before compression was 450 J in a 46 3 cm diameter beam Due to the hole in the paraboloid, 7 4% of the incident energy is lost. The beam was focused using a Cassegrain telescope The primary mirror was a paraboloid (f=180 cm) overcoated with an HfO_2/SiO_2 multilayer designed for high reflectivity at normal incidence The secondary mirror was a 5 cm diameter fused silica flat which was overcoated with a HfO_2/SiO_2 multilayer high reflective coating for 1054 nm and placed 10 cm from the target The beam size on the secondary mirror is 2 6 cm corresponding to an irradiance of 1 67x10^{14} W/cm^2 for a nominal 400 J pulse incident on the mirror At this irradiance, the top SiO_2 layer is converted to a critical density plasma within the first 50 fsec of the pulse As a result, the bulk of the laser pulse is reflected not by the multilayer structure of the mirror but rather by the sharp gradient plasma surface Measurements of the reflectivity from this plasma surface suggest a reflectivity of greater than 85% for the Petawatt pulse Two full scale shots into calorimeters were performed to measure the reflectivity in situ but failed due to difficulties with the Nova data acquisition system

A total of ten Petawatt shots were obtained during this week. Of these, eight were on target and two into calorimeters A typical target is shown in Fig 1. The laser beam strikes the surface of the gold target at near normal (5°) incidence producing a strong relativistic electron current with a complicated angular distribution into the target. Electrons greater than approximately 2 MeV can escape the large space potential created within the target and penetrate the aluminum and CD_2 backing material Electron spectrometers are placed in the plane of incidence

spectrometers are placed in the plane of incidence at 30° from the laser axis and 95° from the axis. These electron spectrometers consist of a permanent dipole magnet with emulsion as the detector. The emulsion tracks are analyzed by the NASA/Marshall Space Flight Center group at Huntsville, Alabama.

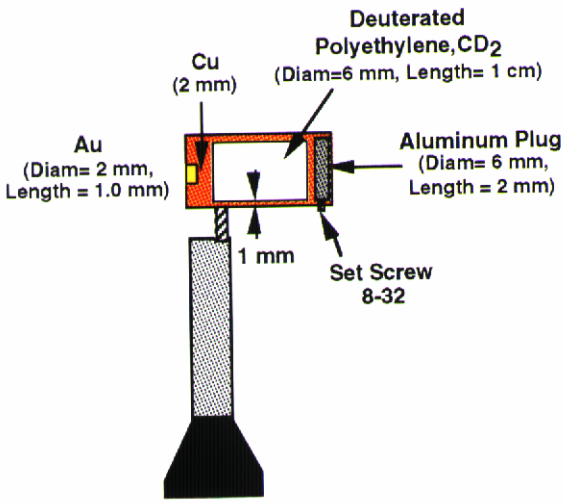

Fig. 1. Petawatt radiography target.

A typical electron spectrum from this shot is shown in Fig. 2. This shot used a gold target of 0.5 mm thickness. Electrons were observed at energies extending above 90 MeV, however the bulk of the distribution was in the range of ~2-15 MeV where the emission was found to be forward directed with about eight times more flux observed at 30°, with respect to the laser propagation direction, as compared to the flux at 95°. Note that an integration of the electron spectrum convolved with the bremsstrahlung cross section does not give an accurate estimate of the total photon yield or laser coupling efficiency since this electron spectrum is effected by the large space charge potential in the target and the energy loss (dE/dx) through the target assembly. The energy loss through the target for the electrons depicted in Fig. 2 was approximately 2.5±0.5 MeV.

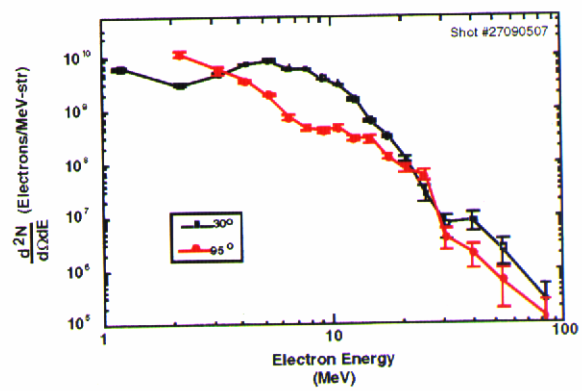

Fig. 2. Electron spectra acquired at 30 and 95 degrees with respect to the laser axis.

Aside from the suppressed region below ≈5 MeV, the electron spectrum can be well fit by a "two temperature" distribution. The spectrum observed at 30 degrees to the laser is shown in Fig.

$$N(E)\,dE = C\,(E^{1/2}/E_e^{3/2})\,\mathrm{Exp}[-E/E_e]\,dE \quad \textbf{(Eq. 1)}$$

where C is the scaling parameter and, E_e is the characteristic electron energy. Detailed particle in cell (PIC) simulations suggest that this characteristic energy is well approximated by the cycle averaged quiver energy of a free electron within the intense field.

$$\langle E_e \rangle = m_e c^2\,[1 + 2U_p/m_e c^2]^{1/2} \quad \textbf{(Eq. 2)}$$

where U_p (eV) = 9.33×10^{-14} I(W/cm^2) λ^2(μm). The laser conditions for the spectrum depicted in Fig. 3 were such that ≈50% of the 300 J incident on the target were focused within a 28x40 μm spot. This corresponds to an average irradiance of 8×10^{19} W/cm^2 for this shot. The average quiver energy for this irradiance (from Eq. 2) is 2.95 MeV in remarkable agreement with the characteristic electron energy for the bulk of the distribution of Fig. 3. The incident laser spot also contained sub-structure which would have seeded self-focusing in the preformed plasma. This self-focusing is almost certainly responsible for the "hot tail" of the distribution characterized by a second Maxwellian with a characteristic electron energy of 11.5 MeV. This is consistent with PIC simulations which show the incident beam undergoing filamentation in the preformed plasma.

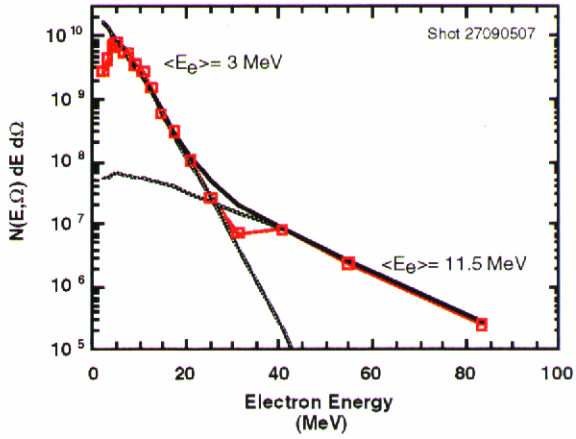

Fig. 3. Electron Spectrum and calculated Maxwellian distributions (Eq. 2). The solid black curve is the sum of the two distributions.

High-energy bremsstrahlung x-rays generated by these electrons in the gold target will produce photonuclear reactions in almost all materials associated with the target assembly and vacuum chamber. The target itself was designed to measure the bremsstrahlung spectrum by measuring the time of flight neutron energy spectrum associated with photodisintegration of deuterium, D(γ,n)H [Q=2.405 MeV]. The hard x-ray yield was so large however that the time of flight neutron scintillator array was overwhelmed by both

scintillator array was overwhelmed by both prompt photons and background neutrons produced in the chamber walls.

Substantial radioactivity was measurable in the target assembly following the laser shot. This activity was due to photonuclear reactions in both the gold and surrounding copper target-holder producing transmutation to platinum and nickel daughter isotopes. The specific reactions observed include $^{197}Au(\gamma,n)^{196}Au$, identified by the decay of the ^{196}Au to ^{196}Pt emitting nuclear gamma-rays at 356 and 333 keV, and $^{63}Cu(\gamma,n)^{62}Cu$ and $^{65}Cu(\gamma,n)^{64}Cu$, which were identified by their subsequent beta decay (positron emission) to ^{62}Ni and ^{64}Ni (Fig. 4). Positron emission was determined by observation of 511 keV γ-rays resulting from annihilation radiation in the target assembly. Positive identification of both copper radioisotopes was established by fitting the decay curve with a two component decay with half-lives of 9.7 min and 12.7 hr (Fig. 4b). The fit gives an identification probability of better than 99% for ^{62}Cu and ^{64}Cu, respectively. The threshold gamma-ray energy for photo-activation of the gold is 8.06 MeV, ^{65}Cu is 9.91 MeV and 10.85 MeV for ^{63}Cu, indicating a large flux of high-energy bremsstrahlung.

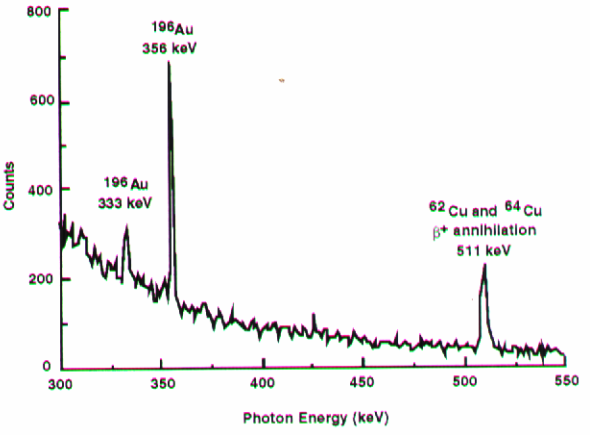

Fig. 4: a. Gamma spectrum of target assembly acquired for ≈30 minutes.

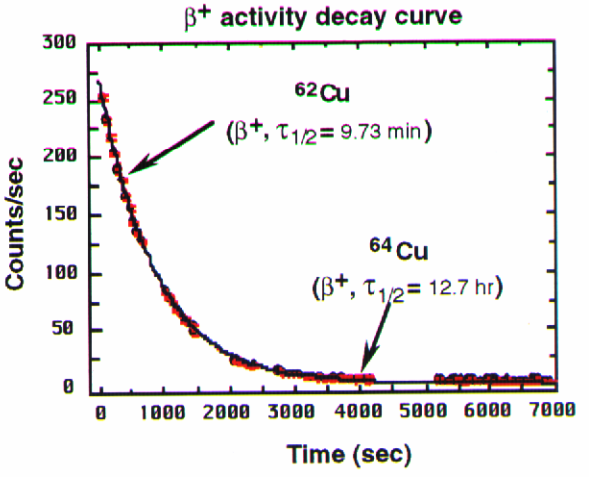

Fig. 4: b. Decay curve of 511 keV annihilation peak with calculated decay curve for isotopic composition of natural copper.

Multiple radiographs thru varying thicknesses of lead were acquired during the shot

series. Two of these, acquired with the film pack placed 81 cm from the target and at 45° to the laser axis, are shown in Figs. 5 and 6. The radiograph in Fig. 5 was acquired on shot 27090808 using tmh film. The depth designation on the figure corresponds to the amount of lead in front of the test object. For depth of 65, 80 and 108 mm, two additional features were machined into the object at 14 mm less depth of Pb. Accounting for the difference in distance between the TLD (100 cm) and the film pack (81 cm), this radiograph would correspond to a dose of >1 MeV photons as measured on the TLD of 0.15 Rad.

The radiograph in Fig. 6 is instructive since on these last two shots, high quality data was obtained from all diagnostics. The film pack was left in the target chamber for shots 27091004, 1006, and 1008. Shot 27091004 was a very strange shot which yielded an inverted electron angular distribution, and low x-ray yield relative to the other shots. The contribution of x-ray output at 45° from this shot relative to 27091006 and 1008 can be neglected. Radiographs corresponding to a difference in film density of >0.2 can be observed through 133 mm of lead ($\rho r \geq 150$ g/cm^2). Due to the attenuation of the lead, only photons with energy greater than approximately 1 MeV contributed to this radiograph. The integrated dose as measured from the TLDs at 100 cm from the target on these shots was: $0.1<E\gamma<0.5$ MeV = 1.6×10^9 photons/cm^2 (0.24 Rads), $0.5<E\gamma<0.8$ MeV = 1.1×10^8 photons/cm^2 (0.03 Rads), $0.8<E\gamma<8$ MeV = 1.7×10^8 photons/cm^2 (0.24 Rads) and $8<E\gamma<20$ MeV = 5.5×10^6 photons/cm^2 (≈.02 Rads).

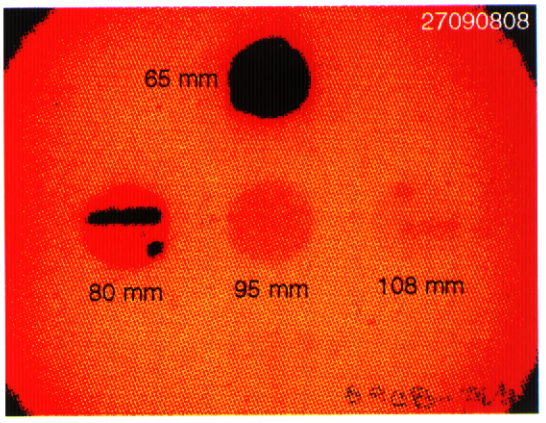

Fig. 5. Radiograph acquired using tmh film at 45° to the laser axis through varying thick-ness of lead attenuator. The film pack was placed 81 cm from the target (Shot 27090808).

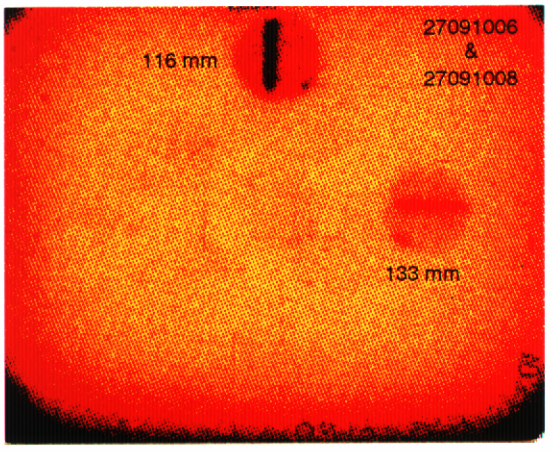

Fig. 6. Radiograph acquired using bmx film at 45° to the laser axis through varying thickness of lead attenuator. The hard x-ray yield from two shots 27091006 and 1008 were summed together on this radiograph.

High quality images of the far-field laser beam distribution were acquired on these shots (Fig. 7). The images show substantial beam distortion resulting from both pump-induced and thermal distortion in the Nova disk amplifiers. This distortion grows throughout the day as the amplifiers heat. Only 9.4 and 10% of the energy is contained within the central 25 μm spot, respectively for the two shots. The pulse energy was ≈280 and 290 J for the shots. As a result, in the absence of self-focusing, the highest irradiance present on target was ≈$2x10^{19}$ W/cm^2. Only the central spot would have had sufficient irradiance to produce the high energy electrons necessary to produce the hard (>1 MeV) x-ray photons. Hence, both the radiograph of Fig. 6 and the TLD spectrum were produced by ≈56 J (sum of energy within the central spot for 27091006 and 1008) focused to an irradiance of ≈ $2x10^{19}$ W/cm^2.

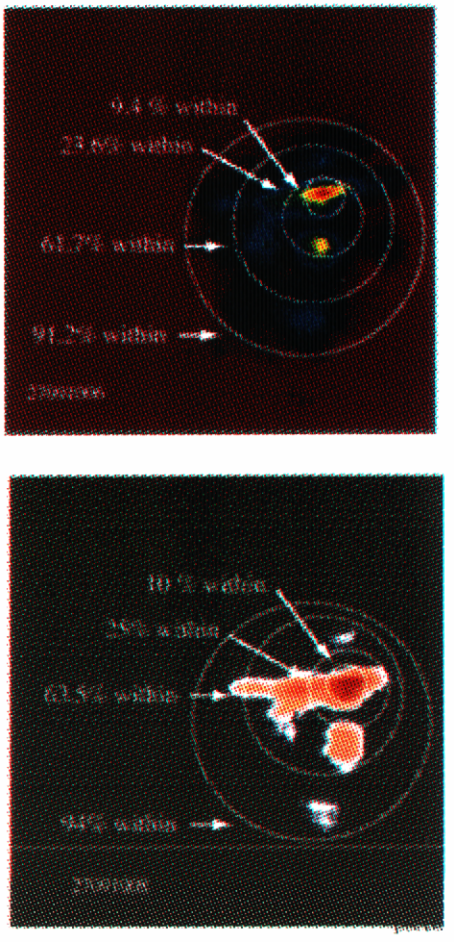

Fig. 7. a) Far-field distribution from shot 27091006 (top) and,
b) shot 27091008 (bottom).

In addition to serving as a testament to the need for the deformable mirror to correct this problem, the far-field data illustrates the need to account for the spatial distribution of irradiance in interpreting any shot data. The electron spectra are relatively insensitive to any portion of the distribution less than $\approx 10^{20}$ W/cm^2 since electrons below ≈3 MeV cannot escape the target as described previously. This is not the case of the bremsstrahlung spectra which will include contributions from all hot electrons in the target. The thin target bremsstrahlung spectra from the electron distributions of Eq. 1 at 10^{19} W/cm^2 ($\langle E_e \rangle$=1 MeV), $\approx 10^{20}$ W/cm^2 ($\langle E_e \rangle$=3 MeV) and $\approx 10^{21}$ W/cm^2 ($\langle E_e \rangle$=10 MeV) and a delta function distribution at E_e=10 MeV are shown in Fig. 8. This figure dramatically illustrates the impact of beam quality on the bremsstrahlung spectrum. *A petawatt pulse focused to a 12 μm diameter spot (10^{21} W/cm^2) will produce more than 100 times the x-ray dose above 2 MeV as the same pulse focused to 10^{19} W/cm^2.*

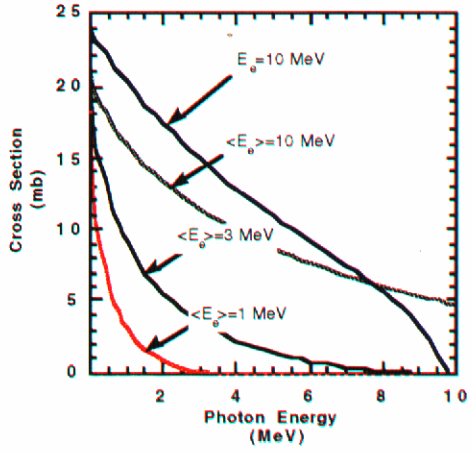

Fig. 8: Thin target bremsstrahlung spectra for the electron distributions of Eq. 1 and the characteristic energies shown. The upper most curve is the calculated spectrum for a monoenergetic 10 MeV electron beam.

In summary, the September shot series was highly successful in providing us our first data on this new type of source. High quality radiographs were obtained through a $\langle \rho r \rangle$ >150 g/cm^2 along with electron spectra extending to 100 MeV and photoactivation of the target assembly. The dose above ≈1 MeV measured using thermoluminescent detectors on the last two shots at 45° and 100 cm from the target was over 0.24 rads. Accounting for the difference in angular distribution (also measured on these shots), this would have

corresponded to 0.6±0 2 rads on axis. From the equivalent plane image, only 10% (56 J) of the incident laser energy was focused to a sufficient irradiance $\approx 2 \times 10^{19}$ W/cm^2 to have contributed to the dose above 1 MeV. As a result of the rapid scaling of the bremsstrahlung output with electron energy and hence laser irradiance, an increase in hard photon yield approaching two orders of magnitude may be achievable by improving the beam quality to enable an irradiance approaching 10^{21} W/cm^2 (800 J in 450 fsec focused to a 15 μm diameter spot, 2x diffraction limited) These conclusions are supported by the large difference in the yield of high energy electrons from an early shot (27090507) with moderate beam quality (>1 6×10^9 e$^-$/MeV-str) compared to that from a later shot with poor beam quality (27091006) $8\ 8 \times 10^7$ e$^-$/MeV-str) both at 30° and 12 5 MeV, a difference of 20. Finally, both in the electron and photon data, there is a strong high energy component which cannot be explained without filamentation of the beam in the preformed plasma resulting in small regions of locally high intensity or the presence of acceleration mechanisms

III. FUTURE WORK

In order to improve the quality of the laser beam, adaptive optics are being incorporated in the Petawatt design A deformable mirror will be placed in the master oscillator room and the beam will be conditioned to compensate for thermal aberrations in the amplifier section of Nova beamline 6 This will improve the intensity of the beam by approximately a factor of seven over the September shot series In addition, the energy of the beam is being increased from approximately 350 joules to 800 joules using the current diffraction gratings This should increase the radiation dose linearly In the long term, a set of compressor diffraction gratings will be sacrificed at a laser input power level of 1 5 kilojoules

Grating development is underway to produce dielectric transmission gratings that will be capable of handling a five kilojoule pulse In addition, a demonstration will be performed on the Beamlet laser (the prototype laser for the National Ignition Facility (NIF)) to extract 2 sequenced pulses at 5 kilojoules each at 1ω within a few nanoseconds of each other The theoretical limit for pulse extraction from Beamlet is approximately 15 kilojoules If all the scaling works as predicted, the potential exists for the production of 50-200 rads at 1 meter or axis from

a Beamlet/Petawatt laser device Further improvements using tailored target design might be possible Finally, because the pulse from a laser radiographic source is so short (<10 psec) compared to electron-beam driven pulses (~60-70 nsec), the use of time-gated imaging systems might allow for the production of a high-definition image because of the elimination of the scattered photon component

ACKNOWLEDGEMENTS

This work was performed under the auspices of the Department of Energy by the Lawrence Livermore National laboratory under Contract W-7405-Eng-48

REFERENCES

1 W. Priedhorsky, D Lier, R Day, and D Gerke, "Hard x-ray measurements of 10 6 micron Laser Irradiated Targets," Physical Review Letters, **47**, 1661 (1981)

2 M D Perry, C Keane, and E M Campbell, "Ultrahigh Brightness Lasers and their Applications," LLNL Internal document (1987)

3 J D Kmetec, C L Gordon, J.J. Macklin, B E Lemoff, and S.E. Harris, "MeV X-ray Generation with Femtosecond Lasers," Physical Review Letters, **68**, 1527 (1992)

4 G Malka and J L Miquel, Physical Review Letters, **77**, 75 (1996).

5 G Malka, E Lefebvre, J L Miquel, and C Rousseaux, "Observation of Relativistic Electrons Produced in the Interaction of 400 Fsec Laser Pulses with Solid Targets," Anomalous Absorption Conference, Fairbanks, Alaska, August 1996

6 P. Gibbon, "Efficient Production of Fast Electrons from Femtosecond Laser Interaction with Solid Targets," Physical Review Letters, **73**, 664 (1994)

Technical Information Department • **Lawrence Livermore National Laboratory**
University of California • Livermore, California 94551